



ELSEVIER

Journal of Chromatography A, 743 (1996) 3–14

JOURNAL OF  
CHROMATOGRAPHY A

# Effects of structural and kinetic parameters on the performance of chromatographic columns packed with perfusive and purely diffusive adsorbent particles

G.A. Heeter, A.I. Liapis\*

Department of Chemical Engineering and Biochemical Processing Institute, University of Missouri-Rolla, Rolla, MO 65401-0249, USA

## Abstract

A mathematical model describing dynamic adsorption in columns with spherical bidisperse perfusive or spherical bidisperse purely diffusive adsorbent particles is used to study the effects of the structural parameters of the adsorbent particles and of the parameters of the adsorption mechanism on the performance of chromatographic systems involving the adsorption of bovine serum albumin onto anion-exchange porous adsorbent particles. Four structural parameters are studied: the particle diameter,  $d_p$ , the macropore void fraction,  $\varepsilon_p$ , the microparticle diameter,  $d_m$ , and the parameter  $\phi$ , which affects the value of the permeability of the adsorbent particle. Two parameters of the adsorption mechanism are studied: the maximum equilibrium concentration of adsorbate in the adsorbed phase of the adsorbent particle,  $C_T$  and the rate constant  $k_1$ , which characterizes the adsorption step of the interaction mechanism between the adsorbate molecules and the active sites on the surface of the pores of the adsorbent particles. The performance of columns packed with purely diffusive particles improves when the value of  $d_p$  is decreased, when the value of  $\varepsilon_p$  is increased and when the value of  $d_m$  is decreased; the effect of  $d_m$  is much smaller than the effects of  $d_p$  and  $\varepsilon_p$ . Intraparticle flow in perfusive particles can improve column performance if it is of sufficient magnitude; intraparticle flow increases when the value of  $d_p$  is decreased, when the value of  $\varepsilon_p$  is increased, when the value of  $d_m$  is increased and when the value of  $\phi$  is decreased. The difference between the performance of a column packed with perfusive particles and that of a column packed with purely diffusive particles will depend upon the particular combination of the parameters  $d_p$ ,  $\varepsilon_p$ ,  $d_m$  and  $\phi$ . When the value of  $k_1$  is small, an increase in  $k_1$  improves column performance. However, when the value of  $k_1$  becomes sufficiently large, further increases have no effect on column performance. Increasing the value of  $C_T$  has a large effect on column performance by increasing the breakthrough time and the mass of adsorbate in the adsorbed phase at breakthrough. The performance of chromatographic systems with purely diffusive particles can be better than the performance of chromatographic systems with perfusive particles, if purely diffusive particles can be made that have higher values of  $C_T$  than otherwise comparable perfusive particles.

**Keywords:** Adsorption; Adsorbents; Perfusive particles; Stationary phases, LC; Diffusive particles; Albumin

## 1. Introduction

The performance of an adsorption chromatographic system is influenced by the parameters that characterize the structure of the adsorbent particles

that are used in the system, as well as by the parameters that characterize the dynamics of the adsorption mechanism and whose values depend upon the immobilized active sites (chemistry) on the surface of the pores of the adsorbent particles. In this work, the effects of these structural and adsorption mechanism parameters on the performance of perfu-

\*Corresponding author.

sion chromatographic systems are studied. As in previous publications [1–9], we define “perfusion chromatography” to refer to any chromatographic system in which the intraparticle velocity,  $v_p$ , is non-zero [1–10].

Liapis et al. [5] and Heeter and Liapis [7] presented a mathematical model that can be used to describe single component liquid adsorption in chromatographic columns packed with spherical perfusive or spherical purely diffusive adsorbent particles having a bidisperse porous structure. Perfusive adsorbent particles with a bidisperse porous structure were considered to be composed of two regions: a macroporous region made by through-pores (macropores) [1,3–5,7–10] in which intraparticle convection and pore diffusion occur and a microporous [4,5,7–9] region made by spherical microparticles (microspheres [4,5,7–9]) in which pore diffusion occurs. Bidisperse purely diffusive adsorbent particles, in which there is no intraparticle convection, were also considered to be composed of a macroporous region and a microporous region [4,5,7–9]. The model expressions [5] for the adsorbent particles include the intraparticle mass transfer mechanisms of convection and diffusion in the macroporous region and diffusion in the microporous region, as well as the mass transfer step involving the interaction between the adsorbate molecules and the active sites on the surface of the micropores.

In this work, the mathematical model of Liapis et al. [5] is used to study the effects of the structural and adsorption mechanism parameters of the adsorbent particles on the performance of perfusion chromatographic systems involving the adsorption of bovine serum albumin (BSA) in columns packed with spherical anion-exchange porous adsorbent particles. The results obtained from columns with perfusive particles are compared with results determined from the same columns when packed with purely diffusive particles.

## 2. Mathematical model

Adsorption is considered to take place from a flowing liquid stream in a fixed bed of spherical bidisperse adsorbent particles under isothermal con-

ditions. The differential mass balance for the adsorbate in the flowing fluid stream is given by Eq. 1 in Ref. [5] and Eqs. 2 and 5 in Ref. [5] provide the initial and boundary conditions for this continuity equation. Eq. 6 in Ref. [5] represents the differential mass balance for the adsorbate in the macroporous region of the adsorbent particle and its initial and boundary conditions are given by Eqs. 19–23 in Ref. [5]. The continuity equation for the adsorbate in the microporous region of the adsorbent particle is given by Eq. 24 in Ref. [5] and its initial and boundary conditions are given by Eqs. 27–30 in Ref. [5].

In order to solve Eq. 24 in Ref. [5], an expression for the accumulation term  $\partial C_{sm}/\partial t$ , which describes the dynamic adsorption mechanism of the adsorbate molecules with the active sites, is required. The expression used in this work represents the dynamics of the adsorption mechanism  $A^* + S \xrightleftharpoons[k_2]{k_1} A^*S$  and is given by Eq. 26 in Ref. [5], which is as follows:

$$\frac{\partial C_{sm}}{\partial t} = k_1 C_{pm}(C_T - C_{sm}) - k_2 C_{sm} \quad (1)$$

This equation represents one possible functional form of the generalized form in Eq. 25 of Ref. [5]. In this form, the dynamics of the adsorption mechanism are defined by three kinetic parameters: the adsorption rate constant,  $k_1$ , the desorption rate constant,  $k_2$ , and the maximum equilibrium concentration of adsorbate in the adsorbed phase of the adsorbent particle,  $C_T$ . It should be noted that, when equilibrium exists between the adsorbate in the micropore fluid and in the adsorbed phase, Eq. 1 results in the Langmuir equilibrium isotherm.

The variables  $v_{pR}$  and  $v_{p\theta}$  in Eq. 6 of Ref. [5] represent the intraparticle velocity components along the  $R$  and  $\theta$  directions, respectively. The expressions for the velocity components  $v_{pR}$  and  $v_{p\theta}$  can be obtained from the theory of Neale et al. [11], who obtained the analytical expressions for the stream functions outside and inside permeable spheres in a packed bed. By using the expression of Neale et al. [11] for the stream function inside the particle, the following [5,7,12] equations for  $v_{pR}$  and  $v_{p\theta}$  are obtained:

$$v_{pR} = V_f \cos \theta \left[ F - \left( \frac{H}{\xi^2} \right) \left( \frac{\sinh \xi}{\xi} - \cosh \xi \right) \right] \quad (2)$$

$$v_{p\theta} = -V_f \sin \theta \left[ F - \left( \frac{H}{2\xi} \right) \times \left( \left( \frac{\xi \cosh \xi - \sinh \xi}{\xi^2} \right) - \sinh \xi \right) \right] \quad (3)$$

The expressions for  $\xi$ ,  $F$  and  $H$  are as follows [11]:

$$\xi = \frac{R}{\sqrt{K_p}} \quad (4)$$

$$F = \frac{B}{\beta^3} + 10D \quad (5)$$

$$H = \frac{1}{J} [6\beta^2(\operatorname{sech} \beta)(1 - \eta^5)] \quad (6)$$

where

$$\beta = \frac{R_p}{\sqrt{K_p}} \quad (7)$$

$$\eta = (1 - \varepsilon)^{1/3} \quad (8)$$

$$J = 2\beta^2 - 3\beta^2\eta + 3\beta^2\eta^5 - 2\beta^2\eta^6 + 90\beta^{-2}\eta^5 + 42\eta^5 - 30\eta^6 + 3 - \frac{\tanh \beta}{\beta}(-3\beta^2\eta + 15\beta^2\eta^5 - 12\beta^2\eta^6 + 90\beta^{-2}\eta^5 + 72\eta^5 - 30\eta^6 + 3) \quad (9)$$

$$B = \frac{1}{J} \left[ 3\beta^3 + 2\beta^3\eta^5 + 30\beta\eta^5 - \frac{\tanh \beta}{\beta}(3\beta^3 + 12\beta^3\eta^5 + 30\beta\eta^5) \right] \quad (10)$$

$$D = -\frac{\eta^5 A}{\beta^5} \quad (11)$$

$$A = -\frac{1}{J} \left[ \beta^5 + 6\beta^3 - \frac{\tanh \beta}{\beta}(3\beta^5 + 6\beta^3) \right] \quad (12)$$

It should be mentioned at this point that the process used to manufacture the porous adsorbent particles could produce a distribution in the sizes (diameters) of the microspheres from which the adsorbent particles are made; in other words, in real adsorbent particles with a bidisperse porous structure and which are made by aggregating microspheres, there is a distribution in the diameters of the microspheres in the porous adsorbent particles. Therefore, it is important to realize that the value of

the diameter,  $d_m$  ( $d_m = 2r_m$ ), of the microsphere in Fig. 1 of Ref. [5] represents the mean value of the distribution of microsphere diameters in the adsorbent particle.

The value of the permeability of the macroporous region,  $K_p$ , in Eq. 4 and Eq. 7 could be estimated from the following approximate expression [5,6,13–16]:

$$K_p = \frac{d_m^2 \varepsilon_p^3}{\phi (1 - \varepsilon_p)^2} \quad (13)$$

In Eq. 13,  $\varepsilon_p$  represents the porosity of the macroporous region. The value of the parameter  $\phi$  could depend upon the shape and packing arrangement of the microparticles and is commonly given as 150 [6,13–16]. However, Eq. (13) with  $\phi = 150$  could overestimate the value of  $K_p$  of the real adsorbent particles because the process of sticking (gluing) the microspheres together in order to form the porous adsorbent particle could (a) reduce the pore connectivity among various macropores and (b) produce macropores that do not interconnect with other macropores; both cases (a) and (b) could increase the value of  $\phi$  and this would make the value of  $K_p$  of the real porous particles lower than if  $\phi$  was equal to 150.

The range of values of the parameters of the system studied in this work is such that the value of  $H$  in Eqs. 2 and 3 is essentially equal to zero [14]. Thus, the values of  $v_{pR}$  and  $v_{p\theta}$ , for the adsorption system studied in this work, are obtained from the following expressions ( $H \approx 0$  in Eqs. 2 and 3):

$$v_{pR} \approx FV_f \cos \theta \quad (14)$$

$$v_{p\theta} \approx FV_f \sin \theta \quad (15)$$

These equations show that the structural parameters of a perfusive particle influence the intraparticle flow solely through the parameter  $F$ ; it is worth noting that when  $F = 0$  the adsorbent particles are purely diffusive (the structure of the particles is such that there is no intraparticle fluid flow); while when  $F > 0$  the adsorbent particles are perfusive. By examining Eq. 5 and Eqs. 7–13, it becomes apparent that the parameter  $F$  depends upon the column void fraction,  $\varepsilon$ , and four structural parameters of the particle: the particle diameter,  $d_p$ , the macropore void fraction,

$\varepsilon_p$ , the microparticle diameter,  $d_m$ , and the parameter  $\phi$  in Eq. 13. In this work, the value of  $\varepsilon$  was held constant at 0.35.

The axial component of the intraparticle velocity,  $v_{px_1}$ , which is parallel to the flowing fluid stream along the axis of the column (see Fig. 1 in Ref. [5]), is given by

$$v_{px_1} = v_{pR} \cos \theta - v_{p\theta} \sin \theta \quad (16)$$

When  $H$  is taken to be approximately equal to zero, and  $v_{pR}$  and  $v_{p\theta}$  are given by Eq. 14 and Eq. 15, respectively, the following expression for  $v_{px_1}$  is obtained:

$$v_{px_1} = FV_f \quad (17)$$

If the intraparticle Peclet number,  $Pe_{intra}$ , could be defined as

$$Pe_{intra} = \frac{v_{px_1} d_p}{D_p} \quad (18)$$

where  $D_p$  represents the effective pore diffusion coefficient of the adsorbate in the pore fluid of the macroporous region, then by using the expression for  $v_{px_1}$  given in Eq. 17, the following expression for  $Pe_{intra}$  is obtained:

$$Pe_{intra} = \frac{FV_f d_p}{D_p} \quad (19)$$

The solution of the model equations for the system studied in this work was obtained by the numerical solution procedure reported in Refs. [5] and [14].

### 3. Results and discussion

In this work, the effects of the structural and kinetic parameters of anion-exchange porous adsorbent particles on the efficiency with which those particles are utilized by the adsorption of BSA in fixed bed column systems were studied. The structural parameters of the adsorbent particles that were varied are the particle diameter,  $d_p$ , the macropore void fraction,  $\varepsilon_p$ , the microparticle diameter,  $d_m$ , and the parameter  $\phi$  in Eq. 13. The kinetic parameters of the adsorbent particles that were varied are the maximum equilibrium concentration of adsorbate in

Table 1

Values of the BSA adsorption system parameters that were varied

Parameter	Values
$C_T$	39.15 kg/m <sup>3</sup> , 78.30 kg/m <sup>3</sup> , 117.45 kg/m <sup>3</sup>
$d_m$	700 Å, 7000 Å, 12 000 Å
$d_p$	15 μm, 30 μm, 50 μm
$D_p^a$	$2.95 \times 10^{-12}$ m <sup>2</sup> /s, $8.85 \times 10^{-12}$ m <sup>2</sup> /s, $13.27 \times 10^{-12}$ m <sup>2</sup> /s, $17.70 \times 10^{-12}$ m <sup>2</sup> /s
$k_1$	0.105 m <sup>3</sup> /kg·s, 1.05 m <sup>3</sup> /kg·s <sup>b</sup>
$k_2^c$	0.0131 s <sup>-1</sup> , 0.131 s <sup>-1</sup>
$\varepsilon_p$	0.10, 0.30, 0.45, 0.60
$\phi$	150, 300 <sup>d</sup>

<sup>a</sup>  $D_p$  varies only due to its dependence on  $\varepsilon_p$ . The four values of  $D_p$  listed correspond with the four values of  $\varepsilon_p$ .

<sup>b</sup> In addition to these two values of  $k_1$ , a case where it is assumed that equilibrium exists between adsorbate in the micropore fluid and in the adsorbed phase at each point in the micropores was considered.

<sup>c</sup>  $k_2$  was changed in tandem with  $k_1$  to keep the value of the adsorption equilibrium constant,  $K = k_1/k_2$ , constant. The two values of  $k_2$  listed correspond with the two values of  $k_1$ .

<sup>d</sup> In addition to these two values of  $\phi$ , the case of purely diffusive particles was considered by setting  $F = 0$ .

the adsorbed phase of the adsorbent particle,  $C_T$ , and the adsorption rate constant,  $k_1$ . The values of these parameters that were used for the simulations of the adsorption system studied in this work are listed in Table 1 and the values of other parameters that were held constant for all simulations are listed in Table 2. For each set of structural and kinetic parameters considered, the superficial velocity in the column,  $V_f$ , was varied over a range of values from 300–5743 cm/h. In earlier work [5,7] in which the effect of  $d_m$  on column performance was studied,  $F$  was held constant when  $d_m$  was varied, implying that the value of the parameter  $\phi$  was changed so as to keep

Table 2

Fixed parameters of the BSA adsorption system

Parameter	Value
$C_{d,in}$	0.10 kg/m <sup>3</sup>
$d_c$	0.01 m
$D_L$	0
$D_{pm}$	$7.08 \times 10^{-12}$ m <sup>2</sup> /s
$K = k_1/k_2$	8.015 m <sup>3</sup> /kg
$L$	0.1 m
$T$	296 K
$\varepsilon$	0.35
$\varepsilon_{pm}$	0.50

$F$  constant when  $d_m$  was varied. In this work, the parameter  $\phi$  was held constant when  $d_m$  was varied. The value of the adsorption equilibrium constant,  $K=k_1/k_2$ , was held constant when  $k_1$  was varied, which means that the value of the desorption rate constant,  $k_2$ , was changed in tandem with  $k_1$ . Furthermore, the value of  $C_{d,in}=0.1 \text{ kg/m}^3$  in Table 2 indicates that the value of the inlet concentration of the adsorbate in the flowing fluid stream remains constant for all times of the adsorption stage, and this implies that the simulation studies of this work examine systems of frontal analysis.

The criteria that were used to compare the performance of different columns are the breakthrough time,  $t_b$ , the mass of adsorbate in the adsorbed phase at breakthrough,  $m_{s,b}$ , and the percentage utilization of the adsorptive capacity of the column. In this work, breakthrough time was defined as the time when the concentration of adsorbate in the column outlet stream becomes equal to 1% of  $C_{d,in}$ . The percentage utilization of the adsorptive capacity of the column is obtained by multiplying the ratio of  $m_{s,b}$  to the total adsorptive capacity of the column, which is defined as the total amount of adsorbate in the adsorbed phase at equilibrium (evaluated with respect to the value of  $C_{d,in}$ ), by 100. The values of  $t_b$  and  $m_{s,b}$  are related because the ratio  $m_{s,b}/t_b$ , which could be considered to represent the overall average rate of adsorption, is constant for a given value of  $V_f$  for the systems studied in this work.

In Figs. 1 and 2, the relationship between the parameter  $F$  and the microparticle diameter,  $d_m$ , is shown, for different values of  $\varepsilon_p$  when  $d_p=15 \mu\text{m}$  and  $\phi=150$  in Fig. 1 and for different values of  $d_p$  and  $\phi$  when  $\varepsilon_p=0.45$  in Fig. 2. The curves in Figs. 1,2 are calculated from Eq. 5. The intraparticle Peclet number,  $Pe_{intra}$ , could be calculated from Eq. 19 for any combination of parameters in this work using the value of  $F$  from Fig. 1 or Fig. 2. For all values of  $\varepsilon_p$ ,  $d_p$  and  $\phi$ , the value of  $F$  is very small (though greater than zero) when the value of  $d_m$  is small and increases exponentially as  $d_m$  is increased. The value of  $d_m$  at which  $F$  becomes significantly different from zero depends upon  $\varepsilon_p$ ,  $d_p$  and  $\phi$ . For example, in Fig. 1,  $F$  rises above zero at a  $d_m$  of about 1000 Å when  $\varepsilon_p=0.60$ , about 2000 Å when  $\varepsilon_p=0.45$ , about 5000 Å when  $\varepsilon_p=0.30$ , and about 40 000 Å when  $\varepsilon_p=0.10$ . The value of  $d_m$  at which

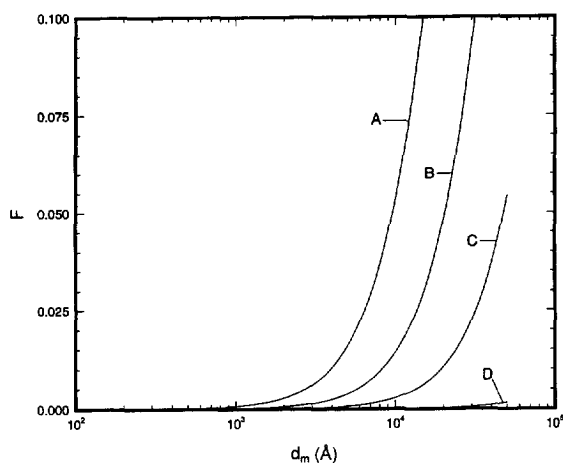


Fig. 1. The dependence of  $F$  on the microparticle diameter for different values of  $\varepsilon_p$  when  $d_p=15 \mu\text{m}$  and  $\phi=150$ . (A)  $\varepsilon_p=0.60$ ; (B)  $\varepsilon_p=0.45$ ; (C)  $\varepsilon_p=0.30$ ; (D)  $\varepsilon_p=0.10$ .

$F$  becomes significantly different from zero also increases when the value of  $d_p$  is decreased and when the value of  $\phi$  is decreased. Consequently, at any given value of  $d_m$ , the value of  $F$  will increase as  $\varepsilon_p$  is increased,  $d_p$  is decreased and  $\phi$  is decreased.

In Fig. 3, the relationship between the percentage utilization of the adsorptive capacity of the column and the superficial velocity in the column is pre-

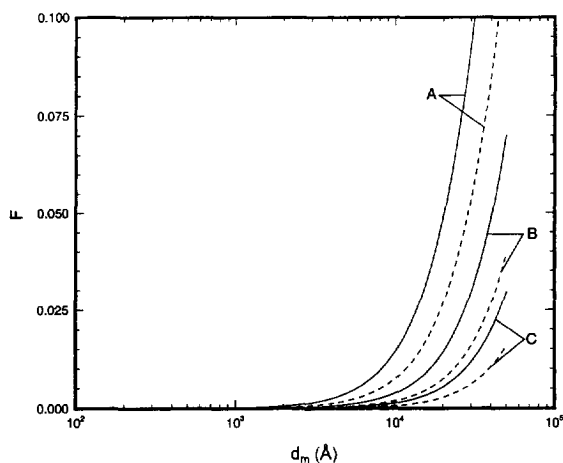


Fig. 2. The dependence of  $F$  on the microparticle diameter for different values of  $d_p$  and  $\phi$  when  $\varepsilon_p=0.45$ . The solid curves are for  $\phi=150$  and the dashed curves are for  $\phi=300$ . (A)  $d_p=15 \mu\text{m}$ ; (B)  $d_p=30 \mu\text{m}$ ; (C)  $d_p=50 \mu\text{m}$ .

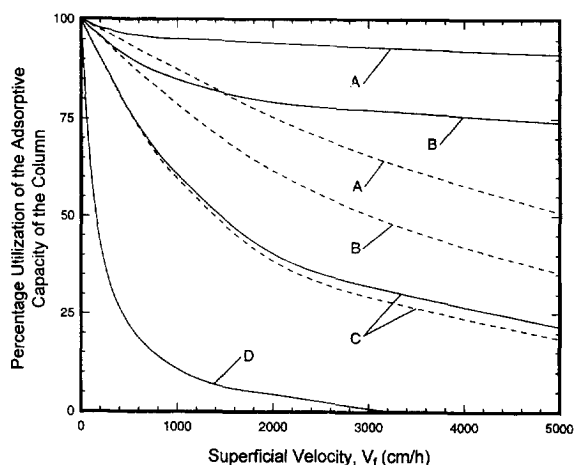


Fig. 3. The percentage utilization of the adsorptive capacity of the column as a function of the superficial velocity for perfusive and purely diffusive particles for different values of  $\varepsilon_p$  when  $d_p = 15 \mu\text{m}$ ,  $d_m = 7000 \text{ \AA}$ ,  $k_1 = 1.05 \text{ m}^3/\text{kg}\cdot\text{s}$ ,  $k_2 = 0.131 \text{ s}^{-1}$  and  $C_T = 78.30 \text{ kg/m}^3$ . The solid curves are for perfusive ( $F > 0$ ,  $\phi = 150$ ) particles and the dashed curves are for purely diffusive ( $F = 0$ ) particles. (A)  $\varepsilon_p = 0.60$ ; (B)  $\varepsilon_p = 0.45$ ; (C)  $\varepsilon_p = 0.30$ ; (D)  $\varepsilon_p = 0.10$ .

sented for different values of the particle macropore void fraction,  $\varepsilon_p$ , for both purely diffusive ( $F = 0$ ) and perfusive ( $F > 0$ ,  $\phi = 150$ ) particles when  $d_p = 15 \mu\text{m}$ ,  $d_m = 7000 \text{ \AA}$ ,  $k_1 = 1.05 \text{ m}^3/\text{kg}\cdot\text{s}$ ,  $k_2 = 0.131 \text{ s}^{-1}$  and  $C_T = 78.30 \text{ kg/m}^3$ . The solid curves represent the results for perfusive particles, while those for purely diffusive particles are denoted by dashed curves; when  $\varepsilon_p = 0.10$ , the curves for perfusive particles and purely diffusive particles coincide. The results show that the percentage utilization increases greatly when the value of  $\varepsilon_p$  is increased, for both perfusive and purely diffusive particles, and the increase in percentage utilization is greater for perfusive particles than for purely diffusive particles. An increase in  $\varepsilon_p$  lowers the resistance to diffusion in the macroporous region of both perfusive and purely diffusive particles, increasing the amount of adsorbate that reaches the microporous region to be adsorbed, thus increasing the percentage utilization. Additionally, an increase in  $\varepsilon_p$  increases the value of  $F$ , and thus, the amount of intraparticle flow in the macroporous region of perfusive particles, further reducing the mass transfer resistance within the macroporous region and increasing the percentage utilization. When  $\varepsilon_p = 0.10$ , there is no difference

between the performance of perfusive and purely diffusive particles, indicating that the magnitude of  $F$ , and therefore the amount of intraparticle flow, is too small to have any significant effect on the mass transfer resistance. When the value of  $\varepsilon_p$  is increased to 0.30,  $F$  is larger, there is more intraparticle flow, and perfusive particles show a small advantage in performance over purely diffusive particles. When  $\varepsilon_p = 0.45$  and  $\varepsilon_p = 0.60$ , not only do perfusive particles perform much better than purely diffusive particles, but also the rate at which the percentage utilization decreases as the superficial velocity increases is greatly reduced for perfusive particles compared to purely diffusive particles.

Fig. 4 shows the relationship between the percentage utilization and the superficial velocity for different values of the adsorbent particle diameter,  $d_p$ , for both purely diffusive ( $F = 0$ ) and perfusive ( $F > 0$ ,  $\phi = 150$ ) particles when  $\varepsilon_p = 0.45$ ,  $d_m = 7000 \text{ \AA}$ ,  $k_1 = 1.05 \text{ m}^3/\text{kg}\cdot\text{s}$ ,  $k_2 = 0.131 \text{ s}^{-1}$  and  $C_T = 78.30 \text{ kg/m}^3$ . The results for perfusive particles are represented by solid curves, while those for purely diffusive particles are denoted by dashed curves. For both perfusive and purely diffusive particles, the percentage utilization increases when the value of  $d_p$

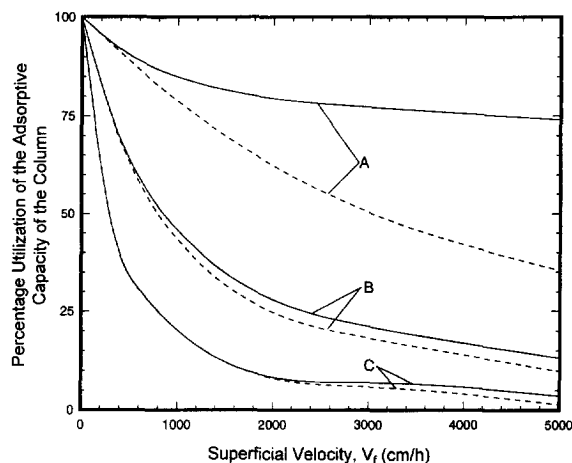


Fig. 4. The percentage utilization of the adsorptive capacity of the column as a function of the superficial velocity for perfusive and purely diffusive particles for different values of  $d_p$  when  $\varepsilon_p = 0.45$ ,  $d_m = 7000 \text{ \AA}$ ,  $k_1 = 1.05 \text{ m}^3/\text{kg}\cdot\text{s}$ ,  $k_2 = 0.131 \text{ s}^{-1}$  and  $C_T = 78.30 \text{ kg/m}^3$ . The solid curves are for perfusive ( $F > 0$ ,  $\phi = 150$ ) particles and the dashed curves are for purely diffusive ( $F = 0$ ) particles. (A)  $d_p = 15 \mu\text{m}$ ; (B)  $d_p = 30 \mu\text{m}$ ; (C)  $d_p = 50 \mu\text{m}$ .

is decreased, because the length of diffusion paths in the macroporous region of the adsorbent particle is reduced when the value of  $d_p$  is decreased. When  $d_p = 50 \mu\text{m}$ , the performance of perfusive particles and that of purely diffusive particles are nearly the same. As  $d_p$  is decreased, the difference between the performance of perfusive and purely diffusive particles increases, because the value of  $F$ , and thus the amount of intraparticle flow, increases as  $d_p$  is decreased.

The relationship between the percentage utilization and the superficial velocity for different values of the microparticle diameter,  $d_m$ , for purely diffusive ( $F = 0$ ) and perfusive ( $F > 0$ ,  $\phi = 150$  and  $\phi = 300$ ) particles, when  $\varepsilon_p = 0.45$ ,  $d_p = 15 \mu\text{m}$ ,  $k_1 = 1.05 \text{ m}^3/\text{kg}\cdot\text{s}$ ,  $k_2 = 0.131 \text{ s}^{-1}$  and  $C_T = 78.30 \text{ kg}/\text{m}^3$ , is shown in Fig. 5. The results for purely diffusive particles are represented by dashed curves; the results for perfusive particles with  $\phi = 150$  are represented by solid curves; and the results for perfusive particles with  $\phi = 300$  are represented by dotted curves. The curves for purely diffusive particles and perfusive particles with  $\phi = 150$  and with  $\phi = 300$  all coincide when  $d_m = 700 \text{ \AA}$ . For purely diffusive particles, there is a

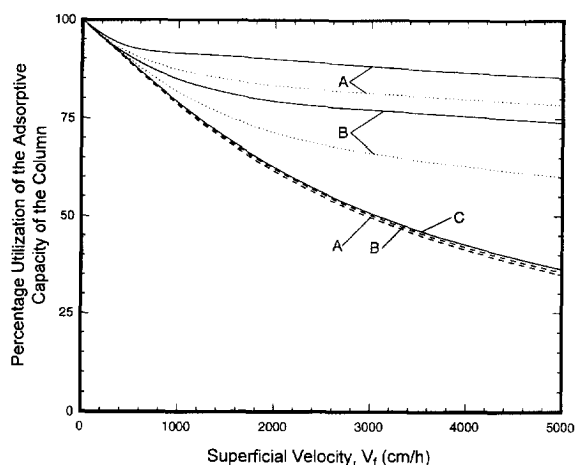


Fig. 5. The percentage utilization of the adsorptive capacity of the column as a function of the superficial velocity for perfusive and purely diffusive particles for different values of  $d_m$  when  $\varepsilon_p = 0.45$ ,  $d_p = 15 \mu\text{m}$ ,  $k_1 = 1.05 \text{ m}^3/\text{kg}\cdot\text{s}$ ,  $k_2 = 0.131 \text{ s}^{-1}$  and  $C_T = 78.30 \text{ kg}/\text{m}^3$ . The solid curves are for perfusive ( $F > 0$ ) particles with  $\phi = 150$ , the dashed curves are for purely diffusive ( $F = 0$ ) particles and the dotted curves are for perfusive ( $F > 0$ ) particles with  $\phi = 300$ . (A)  $d_m = 12\,000 \text{ \AA}$ ; (B)  $d_m = 7\,000 \text{ \AA}$ ; (C)  $d_m = 700 \text{ \AA}$ .

small decrease in the percentage utilization when the value of  $d_m$  is increased, due to the increase in the length of diffusion paths within the microsphere. The effect of changes in  $d_m$  on the performance of columns with purely diffusive particles is much smaller than the effect of changes in  $\varepsilon_p$  and  $d_p$ , indicating that the effect of the mass transfer resistance in the macroporous region of the particle is greater than the effect of the mass transfer resistance in the microporous region. The results in Fig. 5 show that, for perfusive particles, the percentage utilization increases when the value of  $d_m$  is increased. At  $d_m = 700 \text{ \AA}$ , the performance of perfusive and purely diffusive particles are essentially the same; there is not sufficient intraparticle flow to affect the performance because the value of  $F$  is too small, both when  $\phi = 150$  and  $\phi = 300$ . When the microsphere diameter is increased to  $7\,000 \text{ \AA}$  or  $12\,000 \text{ \AA}$ , the improvement in performance due to the increase in the intraparticle flow overcomes the decline in performance due to the increase in the length of diffusion paths in the microparticle. This effect is greater when  $\phi = 150$  than when  $\phi = 300$  because the value of  $F$  is larger at  $\phi = 150$ , as shown in Fig. 3.

Figs. 6 and 7 show the relationship between the percentage utilization and the superficial velocity for

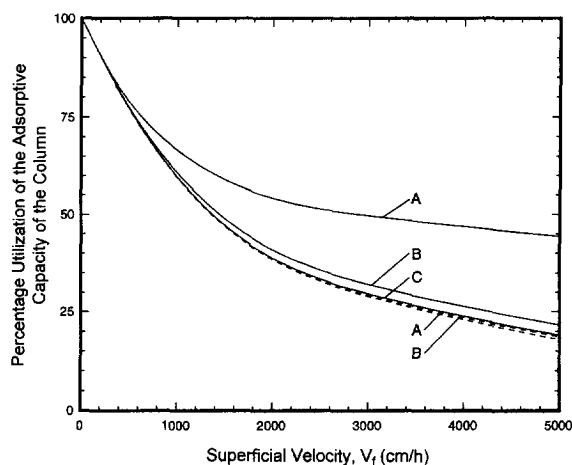


Fig. 6. The percentage utilization of the adsorptive capacity of the column as a function of the superficial velocity for perfusive and purely diffusive particles for different values of  $d_m$  when  $\varepsilon_p = 0.30$ ,  $d_p = 15 \mu\text{m}$ ,  $k_1 = 1.05 \text{ m}^3/\text{kg}\cdot\text{s}$ ,  $k_2 = 0.131 \text{ s}^{-1}$  and  $C_T = 78.30 \text{ kg}/\text{m}^3$ . The solid curves are for perfusive ( $F > 0$ ,  $\phi = 150$ ) particles and the dashed curves are for purely diffusive ( $F = 0$ ) particles. (A)  $d_m = 12\,000 \text{ \AA}$ ; (B)  $d_m = 7\,000 \text{ \AA}$ ; (C)  $d_m = 700 \text{ \AA}$ .

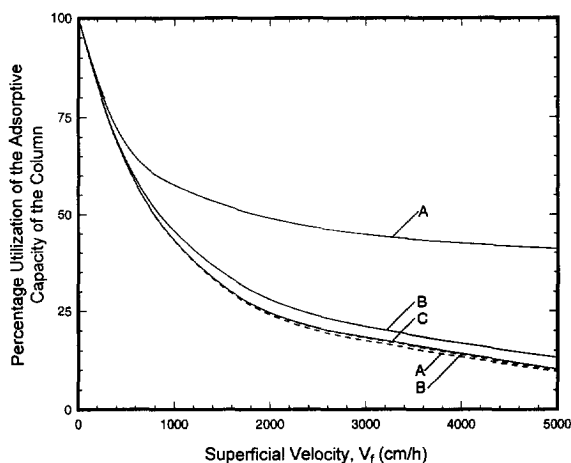


Fig. 7. The percentage utilization of the adsorptive capacity of the column as a function of the superficial velocity for perfusive and purely diffusive particles for different values of  $d_m$  when  $\varepsilon_p = 0.45$ ,  $d_p = 30 \mu\text{m}$ ,  $k_1 = 1.05 \text{ m}^3/\text{kg}\cdot\text{s}$ ,  $k_2 = 0.131 \text{ s}^{-1}$  and  $C_T = 78.30 \text{ kg/m}^3$ . The solid curves are for perfusive ( $F > 0$ ,  $\phi = 150$ ) particles and the dashed curves are for purely diffusive ( $F = 0$ ) particles. (A)  $d_m = 12\,000 \text{ \AA}$ ; (B)  $d_m = 7\,000 \text{ \AA}$ ; (C)  $d_m = 700 \text{ \AA}$ .

different values of the microparticle diameter,  $d_m$ , for purely diffusive ( $F = 0$ ) and perfusive ( $F > 0$ ,  $\phi = 150$ ) particles, when  $\varepsilon_p = 0.30$ ,  $d_p = 15 \mu\text{m}$ ,  $k_1 = 1.05 \text{ m}^3/\text{kg}\cdot\text{s}$ ,  $k_2 = 0.131 \text{ s}^{-1}$  and  $C_T = 78.30 \text{ kg/m}^3$ , and when  $\varepsilon_p = 0.45$ ,  $d_p = 30 \mu\text{m}$ ,  $k_1 = 1.05 \text{ m}^3/\text{kg}\cdot\text{s}$ ,  $k_2 = 0.131 \text{ s}^{-1}$  and  $C_T = 78.30 \text{ kg/m}^3$ , respectively. In both figures, the solid curves represent the results for perfusive particles and the dashed curves denote the results for purely diffusive particles. When  $d_m = 700 \text{ \AA}$ , the curves for purely diffusive particles and perfusive particles coincide. Most features of the results in Figs. 6 and 7 are similar to those of the results in Fig. 5: (1) for purely diffusive particles, there is a decrease in the percentage utilization when the value of  $d_m$  is increased; (2) there is no difference between the performance of perfusive particles and that of purely diffusive particles when  $d_m = 700 \text{ \AA}$ ; and (3) when  $d_m = 7\,000 \text{ \AA}$  or  $d_m = 12\,000 \text{ \AA}$ , perfusive particles perform better than purely diffusive particles. The one different feature is that the magnitude of the difference between the performance of perfusive and purely diffusive particles, when  $d_m = 7\,000 \text{ \AA}$  or  $d_m = 12\,000 \text{ \AA}$ , is much smaller in Figs. 6 and 7 than in Fig. 5. This is because the combinations of parameters in Figs. 6 and 7 result in

smaller values of  $F$  than the combination of parameters in Fig. 5.

The relationship between the percentage utilization and the superficial velocity for two values of the adsorption rate constant,  $k_1$ , and for the case where equilibrium exists between adsorbate in the micropore fluid and in the adsorbed phase at each point in the micropores (infinitely fast kinetics), for purely diffusive ( $F = 0$ ) and perfusive ( $F > 0$ ,  $\phi = 150$ ) particles, when  $\varepsilon_p = 0.45$ ,  $d_p = 15 \mu\text{m}$ ,  $d_m = 7\,000 \text{ \AA}$  and  $C_T = 78.30 \text{ kg/m}^3$  is shown in Fig. 8. The solid curves represent the results for perfusive particles and the dashed curves denote the results for purely diffusive particles. The performance with infinitely fast kinetics is only slightly better than the performance with  $k_1 = 1.05 \text{ m}^3/\text{kg}\cdot\text{s}$  ( $k_2 = 0.131 \text{ s}^{-1}$ ), while there is a large decrease in the percentage utilization when the value of  $k_1$  is reduced to  $0.105 \text{ m}^3/\text{kg}\cdot\text{s}$  ( $k_2 = 0.0131 \text{ s}^{-1}$ ), for both perfusive and purely diffusive particles. These trends have also been found to occur at all other values of  $\varepsilon_p$ ,  $d_p$  and  $d_m$  considered [17]. These results indicate that when  $k_1 = 1.05 \text{ m}^3/\text{kg}\cdot\text{s}$  ( $k_2 = 0.131 \text{ s}^{-1}$ ), the rate of the adsorption step is sufficiently fast to have little effect on the overall mass transfer resistance. However,

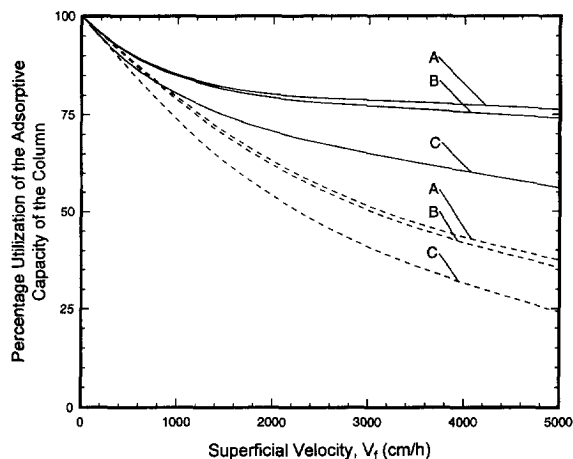


Fig. 8. The percentage utilization of the adsorptive capacity of the column as a function of the superficial velocity for perfusive and purely diffusive particles for different values of  $k_1$ , when  $\varepsilon_p = 0.45$ ,  $d_p = 15 \mu\text{m}$ ,  $d_m = 7\,000 \text{ \AA}$  and  $C_T = 78.30 \text{ kg/m}^3$ . The solid curves are for perfusive ( $F > 0$ ,  $\phi = 150$ ) particles and the dashed curves are for purely diffusive ( $F = 0$ ) particles. (A) infinitely fast kinetics; (B)  $k_1 = 1.05 \text{ m}^3/\text{kg}\cdot\text{s}$  ( $k_2 = 0.131 \text{ s}^{-1}$ ); (C)  $k_1 = 0.105 \text{ m}^3/\text{kg}\cdot\text{s}$  ( $k_2 = 0.0131 \text{ s}^{-1}$ ).



when  $k_1=0.105 \text{ m}^3/\text{kg}\cdot\text{s}$  ( $k_2=0.0131 \text{ s}^{-1}$ ), the contributions of the adsorption step and the mass transfer within the macroporous region of the adsorbent particle to the overall mass transfer resistance are both significant and important.

Fig. 9 shows the relationship between the percentage utilization for different values of the maximum equilibrium concentration of adsorbate in the adsorbed phase of the adsorbent particle,  $C_T$ , for purely diffusive ( $F=0$ ) and perfusive ( $F>0$ ,  $\phi=150$ ) particles, when  $\varepsilon_p=0.45$ ,  $d_p=15 \text{ }\mu\text{m}$ ,  $d_m=7000 \text{ \AA}$ ,  $k_1=1.05 \text{ m}^3/\text{kg}\cdot\text{s}$  and  $k_2=0.131 \text{ s}^{-1}$ . The solid curves represent the results for perfusive particles and the dashed curves denote the results for purely diffusive particles. There is only a very small increase in the percentage utilization when the value of  $C_T$  is increased, for both perfusive and purely diffusive particles. The same trend was found at all other values of  $\varepsilon_p$ ,  $d_p$  and  $d_m$  considered [17]. The increase in percentage utilization is due to an increase in the rate of the adsorption step when  $C_T$  is increased, which can be seen by examining Eq. 1. The increase in percentage utilization is small because the rate of the adsorption step is sufficiently

fast to have little effect on the overall mass transfer resistance.

Although  $C_T$  has little effect upon the percentage utilization, the breakthrough time,  $t_b$ , and the mass of adsorbate in the adsorbed phase at breakthrough,  $m_{s,b}$ , change significantly when the value of  $C_T$  is changed. Fig. 10 shows the relationship between  $t_b$  and  $C_T$  and Fig. 11 shows the relationship between  $m_{s,b}$  and  $C_T$ , for three different values of the column superficial velocity,  $V_f$ , for purely diffusive ( $F=0$ ) and perfusive ( $F>0$ ,  $\phi=150$ ) particles, when  $\varepsilon_p=0.45$ ,  $d_p=15 \text{ }\mu\text{m}$ ,  $d_m=7000 \text{ \AA}$ ,  $k_1=1.05 \text{ m}^3/\text{kg}\cdot\text{s}$  and  $k_2=0.131 \text{ s}^{-1}$ . In both figures, the results for perfusive particles are represented by solid lines and those for purely diffusive particles are represented by dashed lines. The values of  $t_b$  and  $m_{s,b}$  increase linearly as the value of  $C_T$  is increased and are higher for perfusive particles than for purely diffusive particles. The values of  $t_b$  and  $m_{s,b}$  for perfusive particles are about 8% greater than those for purely diffusive particles when  $V_f=1000 \text{ cm/h}$ , about 53% greater when  $V_f=3000 \text{ cm/h}$  and about 110% greater when  $V_f=5000 \text{ cm/h}$ . The values of  $t_b$  and  $m_{s,b}$  increase by about 100% when the value of  $C_T$  is doubled, for both perfusive and purely diffusive

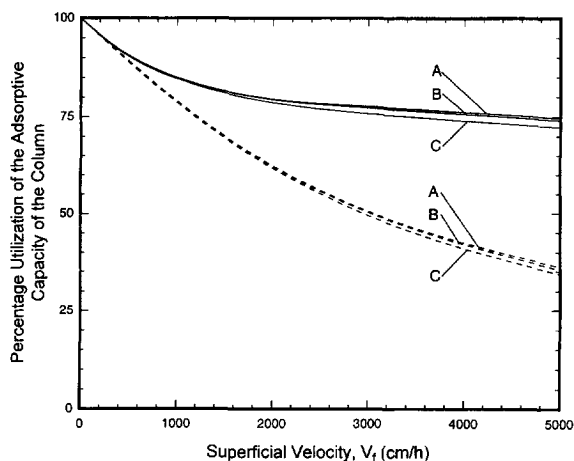


Fig. 9. The percentage utilization of the adsorptive capacity of the column as a function of the superficial velocity for perfusive and purely diffusive particles for different values of  $C_T$  when  $\varepsilon_p=0.45$ ,  $d_p=15 \text{ }\mu\text{m}$ ,  $d_m=7000 \text{ \AA}$ ,  $k_1=1.05 \text{ m}^3/\text{kg}\cdot\text{s}$  and  $k_2=0.131 \text{ s}^{-1}$ . The solid curves are for perfusive ( $F>0$ ,  $\phi=150$ ) particles and the dashed curves are for purely diffusive ( $F=0$ ) particles. (A)  $C_T=117.45 \text{ kg/m}^3$ ; (B)  $C_T=78.30 \text{ kg/m}^3$ ; (C)  $C_T=39.15 \text{ kg/m}^3$ .

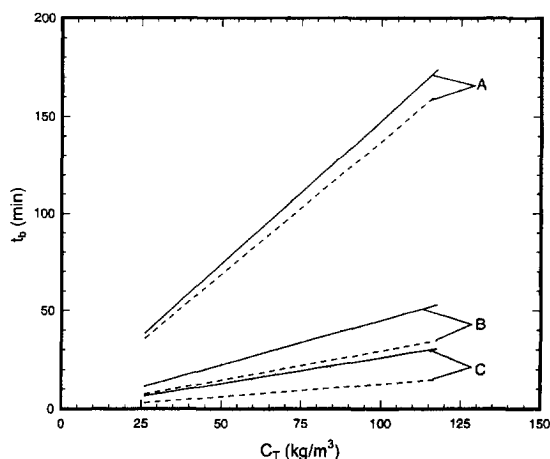


Fig. 10. Breakthrough time,  $t_b$ , as a function of the maximum equilibrium concentration,  $C_T$ , of adsorbate in the adsorbed phase of the adsorbent particle for perfusive and purely diffusive particles for different values of  $V_f$  when  $\varepsilon_p=0.45$ ,  $d_p=15 \text{ }\mu\text{m}$ ,  $d_m=7000 \text{ \AA}$ ,  $k_1=1.05 \text{ m}^3/\text{kg}\cdot\text{s}$  and  $k_2=0.131 \text{ s}^{-1}$ . The solid curves are for perfusive ( $F>0$ ,  $\phi=150$ ) particles and the dashed curves are for purely diffusive ( $F=0$ ) particles. (A)  $V_f=1000 \text{ cm/h}$ ; (B)  $V_f=3000 \text{ cm/h}$ ; (C)  $V_f=5000 \text{ cm/h}$ .

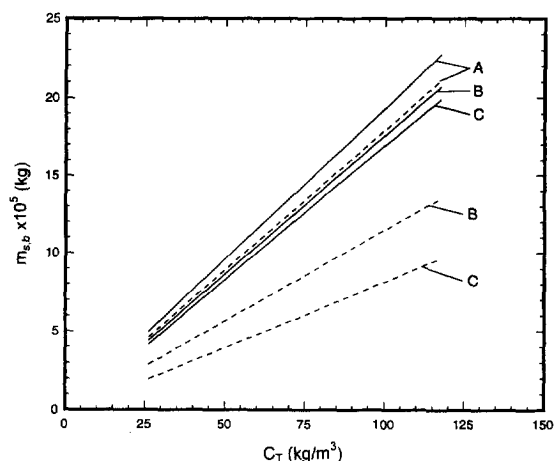


Fig. 11. The mass,  $m_{s,b}$ , of adsorbate in the adsorbed phase at breakthrough as a function of the maximum equilibrium concentration,  $C_T$ , of adsorbate in the adsorbed phase of the adsorbent particle for perfusive and purely diffusive particles for different values of  $V_f$  when  $\epsilon_p=0.45$ ,  $d_p=15\ \mu\text{m}$ ,  $d_m=7000\ \text{\AA}$ ,  $k_1=1.05\ \text{m}^3/\text{kg}\cdot\text{s}$  and  $k_2=0.131\ \text{s}^{-1}$ . The solid curves are for perfusive ( $F>0$ ,  $\phi=150$ ) particles and the dashed curves are for purely diffusive ( $F=0$ ) particles. (A)  $V_f=1000\ \text{cm/h}$ ; (B)  $V_f=3000\ \text{cm/h}$ ; (C)  $V_f=5000\ \text{cm/h}$ .

particles, at all three values of  $V_f$ . Therefore, purely diffusive particles that have high values of  $C_T$  can yield higher values of  $t_b$  and  $m_{s,b}$  than perfusive particles that have low values of  $C_T$ . Increases in  $t_b$  and  $m_{s,b}$  are considered to be improvements in system performance because (a) the adsorption stage makes up a larger portion of the total cycle time, (b) fewer cycles are required to recover a given amount of adsorbate, and (c) the concentration of adsorbate in the column outlet stream during the elution stage could possibly be increased [8]. The performance of chromatographic systems with purely diffusive particles can be better than the performance of chromatographic systems with perfusive particles, if purely diffusive particles can be made that have higher values of  $C_T$  than otherwise comparable perfusive particles; this is shown by the data in Table 3.

#### 4. Conclusions and remarks

A mathematical model of single component adsorption in columns with spherical bidisperse perfu-

Table 3

Performance of chromatographic columns packed with perfusive and purely diffusive adsorbent particles

$V_f$ (cm/h)	$C_T$ (kg/cm <sup>3</sup> )	Perfusive particles ( $F>0$ , $\phi=150$ )			Purely diffusive particles ( $F=0$ )		
		Percentage Utilization	$t_b$ (min)	$m_{s,b}$ (kg)	Percentage Utilization	$t_b$ (min)	$m_{s,b}$ (kg)
300	39.15	93.6	213.6	$8.32 \times 10^{-5}$	93.2	212.7	$8.29 \times 10^{-5}$
	78.30	93.8	426.3	$16.7 \times 10^{-5}$	93.4	424.8	$16.6 \times 10^{-5}$
	117.45	93.9	639.3	$25.0 \times 10^{-5}$	93.5	636.9	$24.9 \times 10^{-5}$
1000	39.15	84.6	57.9	$7.52 \times 10^{-5}$	78.5	53.7	$6.98 \times 10^{-5}$
	78.30	84.9	115.8	$15.1 \times 10^{-5}$	78.7	107.4	$14.0 \times 10^{-5}$
	117.45	85.0	173.7	$22.7 \times 10^{-5}$	79.0	161.4	$21.1 \times 10^{-5}$
3000	39.15	75.8	17.3	$6.74 \times 10^{-5}$	49.5	11.3	$4.40 \times 10^{-5}$
	78.30	77.2	35.1	$13.7 \times 10^{-5}$	50.3	22.9	$8.95 \times 10^{-5}$
	117.45	77.6	52.9	$20.7 \times 10^{-5}$	50.6	34.5	$13.5 \times 10^{-5}$
5000	39.15	72.3	9.9	$6.43 \times 10^{-5}$	34.3	4.7	$3.05 \times 10^{-5}$
	78.30	74.0	20.2	$13.2 \times 10^{-5}$	35.5	9.7	$6.31 \times 10^{-5}$
	117.45	74.6	30.5	$19.9 \times 10^{-5}$	36.2	14.8	$9.65 \times 10^{-5}$

Model parameters:  $t_b$ , breakthrough time;  $m_{s,b}$ , the mass of adsorbate in the adsorbed phase at breakthrough;  $V_f$ , superficial velocity; and  $C_T$ , the maximum equilibrium concentration of adsorbate in the adsorbed phase, for perfusive particles ( $F>0$ ,  $\phi=150$ ) and purely diffusive particles ( $F=0$ ), when  $d_p=15\ \mu\text{m}$ ,  $\epsilon_p=0.45$ ,  $d_m=7000\ \text{\AA}$ ,  $k_1=1.05\ \text{m}^3/\text{kg}\cdot\text{s}$  and  $k_2=0.131\ \text{s}^{-1}$

sive or spherical bidisperse purely diffusive adsorbent particles was used to study the effects of the structural and kinetic parameters of the adsorbent particles on the performance of chromatographic columns, as measured by the percentage utilization of the adsorptive capacity of the column. Four structural parameters,  $d_p$ ,  $\varepsilon_p$ ,  $d_m$  and  $\phi$ , and two kinetic parameters,  $k_1$  and  $C_T$ , were studied. Results from systems with perfusive particles were compared with results from systems with purely diffusive particles.

The structural parameters of purely diffusive particles affect column performance by changing the resistance to diffusion. The values of the parameters  $\varepsilon_p$  and  $d_p$  affect diffusional resistance in the macroporous region of the adsorbent particle, while  $d_m$  affects diffusional resistance in the microporous region. Increases in  $\varepsilon_p$ , decreases in  $d_p$ , and decreases in  $d_m$  all cause increases in the percentage utilization. However, the effect of  $d_m$  is much smaller than the effects of  $\varepsilon_p$  and  $d_p$  because the contribution of the diffusional resistance in the macroporous region to the overall mass transfer resistance of the adsorbent particle is larger than that of the diffusional resistance in the microporous region.

In perfusive particles, the structural parameters affect column performance by changing the amount of intraparticle flow as well as the resistance to diffusion. Intraparticle flow, if it is of sufficient magnitude, can improve column performance by increasing mass transfer within the macroporous region of a perfusive particle. There is no difference between the percentage utilization of perfusive particles and that of purely diffusive particles when  $d_m = 700 \text{ \AA}$  because the value of  $F$ , and therefore the amount of intraparticle flow, is too small to significantly affect the mass transfer within the macroporous region. When  $d_m = 7000 \text{ \AA}$  or  $d_m = 12\,000 \text{ \AA}$ , perfusive particles perform better than purely diffusive particles and the difference between the performance of a column packed with perfusive particles and that of a column packed with purely diffusive particles with the same  $\varepsilon_p$ ,  $d_p$  and  $d_m$  will depend upon the value of  $F$  produced by the particular combination of parameters  $d_p$ ,  $\varepsilon_p$ ,  $d_m$  and  $\phi$ .

An increase in  $k_1$  increases the percentage utilization unless the value of  $k_1$  is sufficiently large that

the rate of the adsorption step is fast enough that it has little effect on the overall mass transfer resistance. An increase in the value of  $C_T$  causes a small increase in percentage utilization and large increases in the breakthrough time,  $t_b$ , and the mass of adsorbate in the adsorbed phase at breakthrough,  $m_{s,b}$ . Increasing the value of  $C_T$  can increase the values of  $t_b$  and  $m_{s,b}$  more than changing from purely diffusive to perfusive particles. The values of  $t_b$  and  $m_{s,b}$  are important in determining the system performance, because when  $t_b$  and  $m_{s,b}$  are increased (a) the adsorption stage makes up a larger portion of the total cycle time, (b) fewer cycles are required to recover a given amount of adsorbate, and (c) the concentration of adsorbate in the column outlet stream during the elution stage could possibly be increased [8]. If purely diffusive particles can be made that have a higher value of  $C_T$  than otherwise comparable perfusive particles, the purely diffusive particles could provide an overall better system performance.

The results presented in this work indicate that the important mass transfer effects occur in the macroporous region of the adsorbent particle. Therefore, for a given particle size, it is important to have high values of  $\varepsilon_p$  and  $F$  in order to achieve good column performance. It is also important to have high values of  $C_T$ . It should be pointed out that the process by which the adsorbent particles are manufactured will place constraints on the values and ranges of values of these parameters. The optimum adsorbent particle construction can be found only by combining modeling results with knowledge of the manufacturing process.

## 5. List of symbols

$A$	parameter given by Eq. 12
$A^*$	adsorbate molecule
$A^*S$	adsorbate-active site complex
$B$	parameter given by Eq. 10
$C_{d,in}$	concentration of adsorbate at $x < 0$ when $D_L \neq 0$ , or at $x = 0$ when $D_L = 0$ , $\text{kg/m}^3$ of bulk fluid
$C_{pm}$	concentration of adsorbate in the fluid of the micropores, $\text{kg/m}^3$ of micropore volume
$C_{sm}$	concentration of adsorbate in the adsorbed

	phase of the microparticle, $\text{kg}/\text{m}^3$ of adsorbent particle
$C_T$	maximum equilibrium concentration of adsorbate in the adsorbed phase of the adsorbent particle, $\text{kg}/\text{m}^3$ of adsorbent particle
$d_c$	diameter of column, m
$d_m$	diameter of spherical microparticle, m
$d_p$	diameter of spherical porous adsorbent particle, m
$D$	parameter given by Eq. 11
$D_L$	axial dispersion coefficient of adsorbate, $\text{m}^2/\text{s}$
$D_p$	effective pore diffusion coefficient of adsorbate in the macropores, $\text{m}^2/\text{s}$
$D_{pm}$	effective pore diffusion coefficient of adsorbate in the micropores, $\text{m}^2/\text{s}$
$F$	parameter given by Eq. 5
$H$	parameter given by Eq. 6
$J$	parameter given by Eq. 9
$k_1$	adsorption rate constant in Eq. 1, $\text{m}^3$ of micropore volume/ $\text{kg}\cdot\text{s}$
$k_2$	desorption rate constant in Eq. 1, $\text{s}^{-1}$
$K$	equilibrium adsorption constant of adsorbate, $K=k_1/k_2$ , $\text{m}^3/\text{kg}$
$K_p$	particle permeability, $\text{m}^2$
$L$	column length, m
$m_{s,b}$	mass of adsorbate in the adsorbed phase at breakthrough, kg
$Pe_{\text{intra}}$	intraparticle Peclet number, dimensionless
$r_m$	radius of microparticle, m
$R$	radial distance in adsorbent particle, m
$R_p$	radius of adsorbent particle, m
$S$	active site
$t$	time, s
$t_b$	breakthrough time, s
$T$	temperature, K
$v_p$	intraparticle velocity vector, m/s
$v_{pR}$	intraparticle velocity component along the $R$ direction, m/s
$v_{p\theta}$	intraparticle velocity component along the $\theta$ direction, m/s
$v_{px_1}$	axial component of the intraparticle velocity, m/s
$V_f$	column fluid superficial velocity, m/s

$\beta$	parameter given by Eq. 7
$\varepsilon$	void fraction in column
$\varepsilon_p$	macropore void fraction
$\varepsilon_{pm}$	micropore void fraction
$\eta$	parameter given by Eq. 8
$\theta$	polar coordinate angle, radians
$\xi$	parameter given by Eq. 4
$\phi$	parameter in Eq. 15

### Acknowledgments

The authors gratefully acknowledge partial support of this work by Monsanto.

### References

- [1] A.I. Liapis and M.A. McCoy, *J. Chromatogr.*, 599 (1992) 87.
- [2] M.A. McCoy, A.I. Liapis and K.K. Unger, *J. Chromatogr.*, 644 (1993) 1.
- [3] A.I. Liapis, *Math. Model. Sci. Comput.*, 1 (1993) 397.
- [4] A.I. Liapis and M.A. McCoy, *J. Chromatogr. A*, 660 (1994) 85.
- [5] A.I. Liapis, Y. Xu, O.K. Crosser and A. Tongta, *J. Chromatogr. A*, 702 (1995) 45.
- [6] A.I. Liapis and K.K. Unger, in G. Street (Editor), *Highly Selective Separations in Biotechnology*, Blackie Academic and Professional, Glasgow, 1994, pp. 121–162.
- [7] G.A. Heeter and A.I. Liapis, *J. Chromatogr. A*, 711 (1995) 3.
- [8] Y. Xu and A.I. Liapis, *J. Chromatogr. A*, 724 (1996) 13.
- [9] G.A. Heeter and A.I. Liapis, *J. Chromatogr. A*, 734 (1996) in press.
- [10] N.B. Afeyan, N.F. Gordon, I. Mazsaroff, L. Varady, S.P. Fulton, Y.B. Yang and F.E. Regnier, *J. Chromatogr.*, 519 (1990) 1.
- [11] G. Neale, N. Epstein and W. Nader, *Chem. Eng. Sci.*, 28 (1973) 1865.
- [12] G. Carta, M.E. Gregory, D.J. Kirwan and H.A. Massaldi, *Sep. Technol.*, 2 (1992) 62.
- [13] M.A. McCoy, Ph.D. Dissertation, Department of Chemical Engineering, University of Missouri-Rolla, Rolla, MO, 1992.
- [14] Y. Xu, Ph.D. Dissertation, Department of Chemical Engineering, University of Missouri-Rolla, Rolla, MO, 1995.
- [15] A.E. Rodrigues, J.C. Lopes, Z.P. Lu, J.M. Loureiro and M.M. Dias, *J. Chromatogr.*, 590 (1992) 93.
- [16] R.B. Bird, W.E. Stewart and E.N. Lightfoot, *Transport Phenomena*, Wiley, New York, NY, 1960.
- [17] G.A. Heeter, Internal Report No. 2, Department of Chemical Engineering, University of Missouri-Rolla, Rolla, MO, 1995.